

TiO₂ coatings on titanium obtained by anodising in a 2% Na₂SiO₃ solution at various voltages

W. Jastrzębski ^{a,*}, M. Wilk ^a, L. Klimek ^b, B. Śmielak ^c


^a Department of Dental Techniques, Medical University of Lodz,
ul. Pomorska 251, 92-231 Łódź, Poland

^b Institute of Material Science and Engineering, Lodz University of Technology,
ul. Stefanowskiego 1/15, 90-924 Łódź, Poland

^c Department of Dental Prosthodontics, Medical University of Lodz,
ul. Pomorska 251, 92-231 Łódź, Poland

* Corresponding e-mail address: wojciechjastrzebski@tlen.pl

ORCID identifier:  <https://orcid.org/0000-0003-0703-3983> (W.J.);

 <https://orcid.org/0000-0003-3617-8225> (L.K.);  <https://orcid.org/0000-0003-2758-0298> (B.Ś.)

ABSTRACT

Purpose: Commercially pure titanium is recognised as one of the most biocompatible materials used in everyday medicine, particularly in prosthodontics. However, its high reactivity with oxygen and low thermal expansion makes titanium difficult to process, making it less popular as a material for porcelain fused to metal substructures. Analysing the available literature studies, both positive and negative effects of the oxide layer on the titanium-ceramic bond have been found. The given work attempted to anodically create oxide coatings in a 2% Na₂SiO₃ solution on commercially pure titanium, which could serve as substructures for crowns and dental bridges.

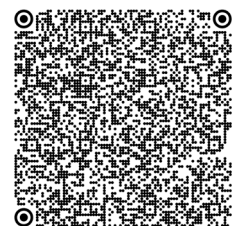
Design/methodology/approach: Grade 2 titanium discs (diameter 20 mm, height 5 mm) were ground and polished. The alloy composition was determined by X-ray fluorescence analysis. The samples were divided into six groups and subjected to anodic oxidation in a 2% Na₂SiO₃ solution at constant voltages: 230 V, 270 V, 300 V, 350 V, 400 V, and a time of t = 1 min. The obtained oxide layers were examined by X-ray diffraction, chemical composition analysis, and SEM observation.

Findings: Coating thicknesses ranging from 0.65 μm to 13.2 μm were obtained. Besides titanium oxide, an amorphous phase is present in the anodised layer.

Research limitations/implications: It is crucial to provide the ideal voltage directly related to the employed solution to maintain the useable thickness of the oxide layers. Variations in oxide layer thickness beyond optimal value may lead to exfoliating if it exceeds 1 μm or present fractures if it subceeds 1 μm.

Originality/value: Titanium oxide layers obtained by anodic oxidation are mainly tested on their biocompatibility and tissue integration so important in implantology. However, the given paper focuses on creating oxide layers that may strengthen the bond between titanium and dental ceramics.

Keywords: Titanium, Dental ceramics, Anodising, Passivation



Reference to this paper should be given in the following way:

W. Jastrzębski, M. Wilk, L. Klimek, B. Śmielak, TiO₂ coatings on titanium obtained by anodising in a 2% Na₂SiO₃ solution at various voltages, Journal of Achievements in Materials and Manufacturing Engineering 120/2 (2023) 75-83. DOI: <https://doi.org/10.5604/01.3001.0054.1478>

BIOMEDICAL AND DENTAL ENGINEERING AND MATERIALS**1. Introduction**

Currently, we are witnessing rapid development in the field of medicine, including dentistry. It is driven by continuous efforts to find better materials and improve their processing technologies. The introduction of 3D printing technology has made it possible to reduce the time and labour required to produce prosthetics or orthodontic appliances [1]. Alongside 3D printing, there is also an increasing interest in biocompatibility, which is receiving considerable attention [2,3]. Not only the proper selection of materials but also their appropriate combination or pairing influences the potential occurrence of allergies or irritations [4-8]. Commonly used Ni-Cr and Co-Cr alloys, employed in the production of crowns and dental bridges, have a negative impact on periodontal tissues. Therefore, continuous efforts are made to address the problem of metal ion release, bacterial plaque accumulation, and subsequent periodontal inflammation [9,10].

Titanium, valued for its unique properties [11], finds applications in various sectors of the economy, including both service and industrial sectors, as well as general medicine and dentistry. Commercially pure titanium, containing over 99% Ti, is considered one of the most biocompatible materials, mainly due to its resistance to corrosion processes. Such resistance arises from forming oxide layers on its surface, primarily TiO₂, through passivation [12]. Thanks to the presence of oxides on its surface, titanium elements integrate perfectly with the body's tissues, even without additional treatment. For aesthetic reasons, titanium crowns require ceramic veneering, which poses a challenge. The high reactivity of titanium with oxygen, low thermal expansion, and passivation make it difficult to achieve adhesion between titanium and ceramics [13]. Thermal processing, commonly used for nickel-chromium and cobalt-chromium alloys, is unsuitable for

titanium due to its reactivity and difficulty in obtaining a homogeneous oxide layer below 1 µm [14,15]. Alternatively, to improve the bond with dental porcelain, the surface can be subjected to abrasive or electrolytic treatment [16]. The latter method is successfully used in dental implants while maintaining full biocompatibility. Similar results on fixed prosthodontic appliances can be achieved with anodised titanium but in a controlled manner [17]. The process is usually conducted in sulfuric or orthophosphoric acids with various modifications [8-20]. To fulfil their function, the produced oxide layers should have an appropriate thickness, i.e., 1 µm, along with a well-developed surface.

2. Aim of research

Due to the beneficial effect of oxide layers on the bond with ceramics, an attempt was made to electrochemically create oxide layers on samples of commercially pure titanium, which served as the substructure for prosthetic restorations.

3. Material and methods

For the purposes of this study, cylindrical titanium samples (commercially pure titanium, Grade II) with a diameter of 20mm and a height of 5mm were utilised. The chemical composition of the samples was analysed using an ARL PERFORM'X X-ray spectrometer from THERMO SCIENTIFIC, and the results were presented in Table 1. Subsequently, the sample bases were wet ground using a rotating grinder with progressively increasing grit sizes: 180, 360, 600, 800, 1200, 2400, and 4000. The samples were divided into six groups based on the applied voltage during the oxidation process.

Table 1.

Chemical composition of the titanium samples used in the study, weight %

Element	Al	Mo	Si	Sn	V	Fe	Ni	W	Ti
Content	0.009	0.002	0.096	0.032	0.017	0.149	0.012	0.019	rest

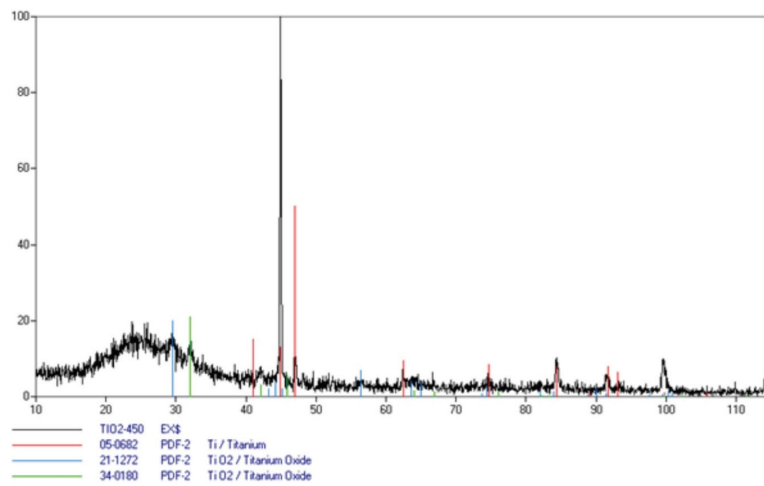


Fig. 1. X-ray diffraction pattern of the sample at 450V

Before the anodising process, the samples were degreased for 5 minutes in a bath with the following composition:

- Na_2CO_3 – 60g/dm³,
- NaOH – 40g/dm³,
- Na_3PO_4 – 30g/dm³,

followed by rinsing with running water.

The prepared samples underwent anodic oxidation in a 2% Na_2SiO_3 (sodium metasilicate) solution with a pH of 13.1 for 1 minute at different current voltages: 230 V, 270 V, 300 V, 350 V, 400 V, and 450 V.

After the anodising process, the samples were subjected to the following analyses:

1. X-ray diffraction (XRD): to determine the phase composition of the anodised layer, XRD analysis was performed using a PANalytical Empyrean X-ray diffractometer.
2. Depth profiling of elemental distribution: to determine changes in the chemical composition within the layer and to assess the thickness of individual layers, a Glow Discharge Optical Emission Spectroscopy (GDOES) analysis was conducted using a LECO GDOES 750 instrument.
3. Scanning Electron Microscopy (SEM) analysis of oxidised surfaces and cross-sections: the morphology of the obtained layers was examined using a Hitachi S-3000N scanning electron microscope.
4. Profilometric analysis: surface profiling was performed using a Mitotuyo SJ-410 stylus profilometer and dedicated software.
5. Measurement of surface free energy using the Owens-Wendt method: The surface free energy of the samples was determined using the Owens-Wendt method.

4. Results and discussion

Figure 1 represents an example X-ray diffraction pattern of the oxide layer from the sample in group number 6.

The diffraction patterns from the remaining groups were similar, with differences primarily in intensity resulting from varying coating thicknesses. In addition to the reflections from the titanium oxide coating, the diffraction patterns also showed reflections from the underlying titanium substrate.

Figures 2-7 represent elemental distributions across the cross-sections of individual layers.

Presented charts reveal the presence of silicon in the anodised layer, alongside with oxygen and titanium. It is due to the use of a 2% Na_2SiO_3 anodising bath. The obtained charts determined the thicknesses of the layers obtained at different anodising voltages. The results are presented in Table 2.

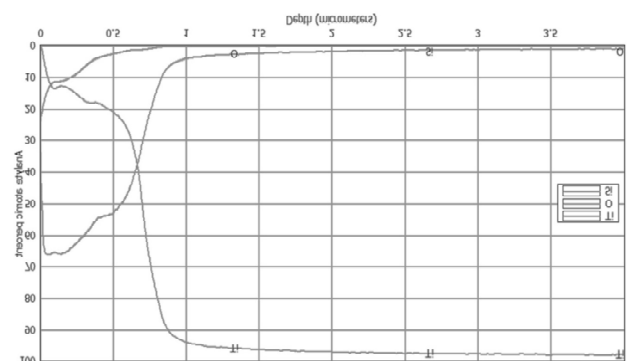


Fig. 2. Elemental distribution in the oxide layer for the sample anodized at 230 V

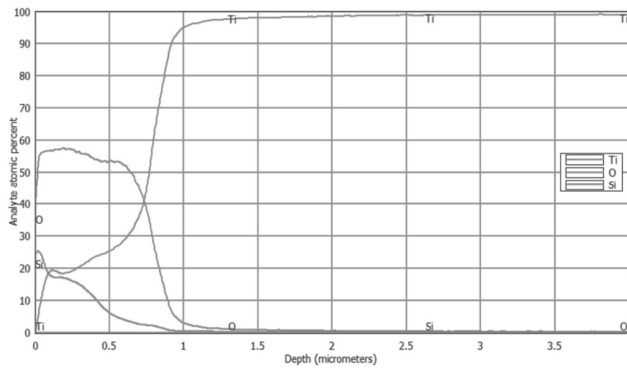


Fig. 3. Elemental distribution in the oxide layer for the sample anodized at 270 V

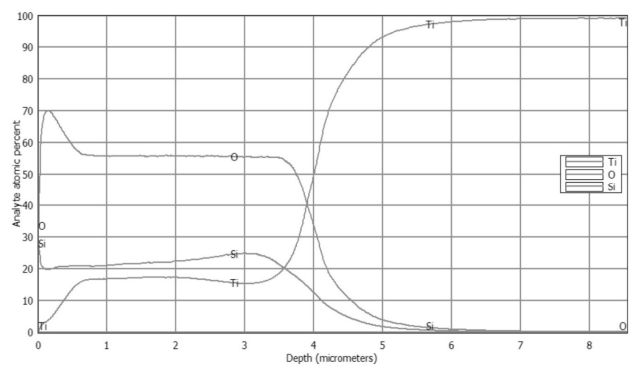


Fig. 6. Elemental distribution in the oxide layer for the sample anodized at 400 V

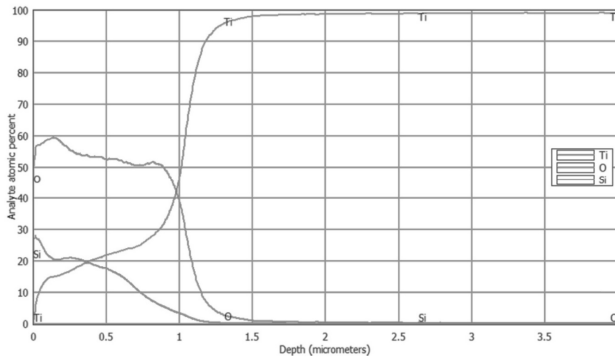


Fig. 4. Elemental distribution in the oxide layer for the sample anodized at 300 V

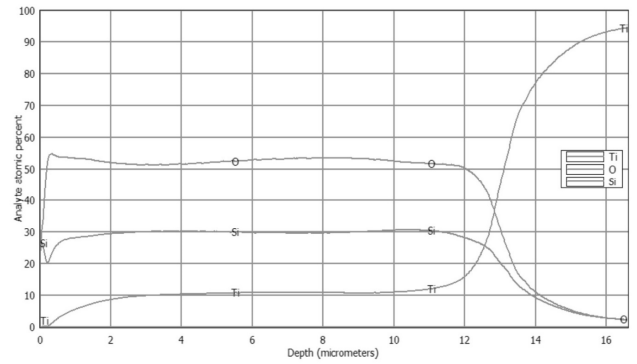


Fig. 7. Elemental distribution in the oxide layer for the sample anodized at 450 V

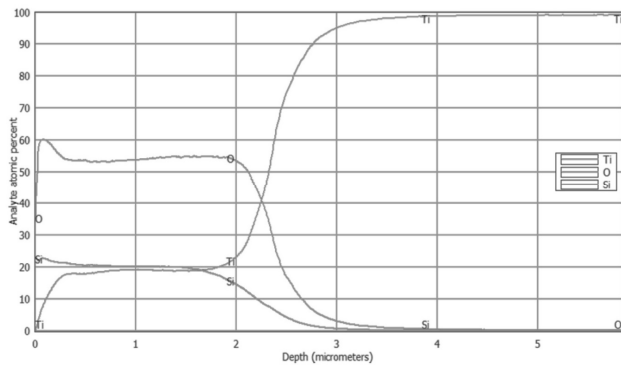


Fig. 5. Elemental distribution in the oxide layer for the sample anodized at 350 V

Table 2.

Thickness of oxide layers for each anodising voltage

Anodising voltage, V	230	270	300	350	400	450
Layer thickness, μm	0.65	0.8	1	2.5	4.6	13.2

Figure 8 shows microscopic images of the surface of the obtained layers, while Figure 9 depicts microscopic images of cross-sections of the obtained layers.

Microscopic images reveal the topography along with the determination of the size and shape of the formed porosities on the oxidised surfaces of titanium. With increasing voltage, the formation of layers with larger porosities, more indentations and undercuts can be observed.

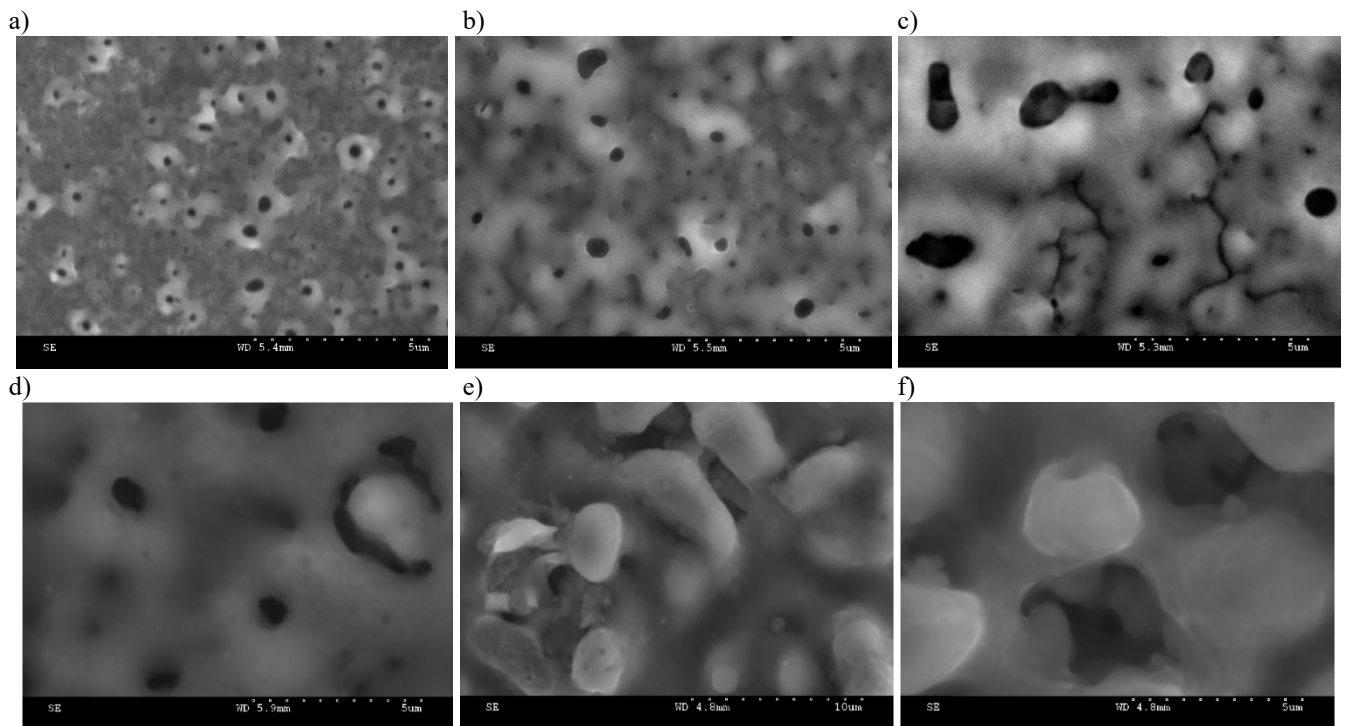


Fig. 8. Microscopic images of the surface of individual samples at: a) 230 V, b) 270 V, c) 300 V, d) 350 V, e) 400 V, f) 450 V

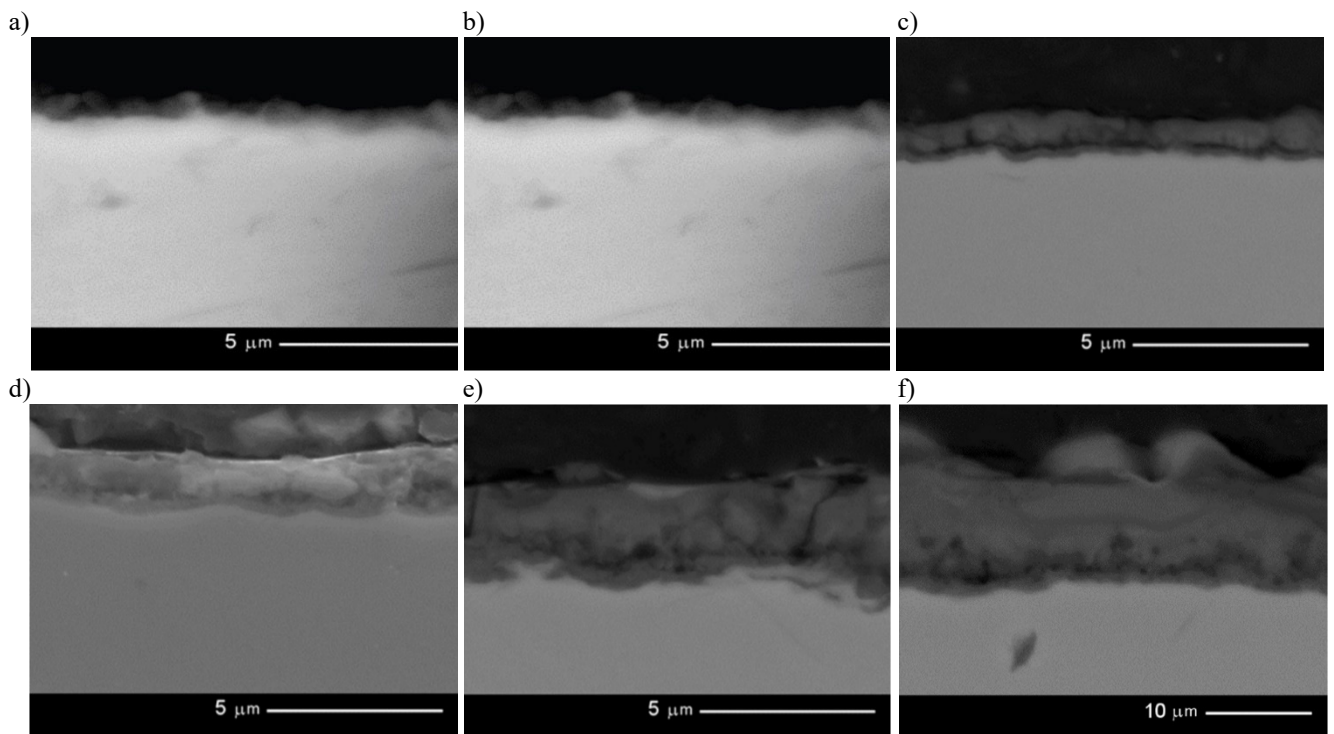


Fig. 9. Microscopic images of cross-sections of individual samples at different anodising voltages: a) 230 V, b) 270 V, c) 300 V, d) 350 V, e) 400 V, f) 450 V

Based on the microscopic images of the cross-sections of individual samples, it is possible to determine the layer thickness, which is comparable to the thickness determined by GDOES analysis, as well as its structure. Porosity of the layers is observed throughout their cross-sections, with the coating growing both above the titanium surface and into the metal.

Figures 10-16 present profiles of the oxide layer heights for the investigated samples, while Table 3 presents numerical values of selected roughness profile parameters for each investigated sample.

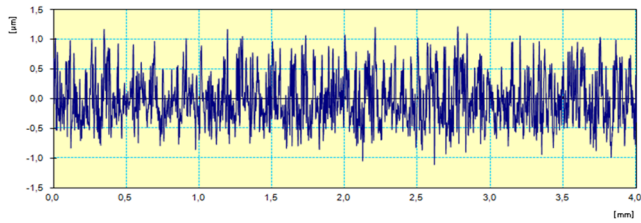


Fig. 10. Exemplary surface roughness profile plot of the samples after anodisation at 200 V

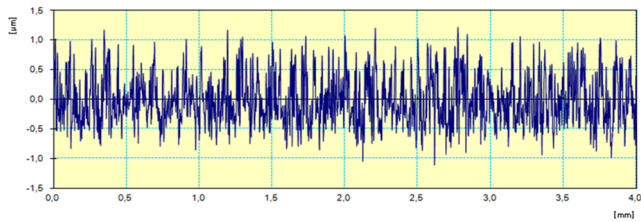


Fig. 11. Exemplary surface roughness profile plot of the samples after anodisation at 230 V

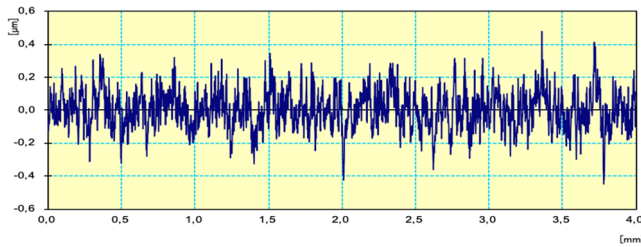


Fig. 12. Exemplary surface roughness profile plot of the samples after anodisation at 270 V

The presented roughness profiles vary depending on the anodising layer. Both the height of the irregularities and the width of the formed indentations differ. It can be observed that the anodised coatings formed at higher anodising voltages exhibit higher roughness profiles, indicating greater thickness of those layers. Those observations are consistent with the microscopic examinations.

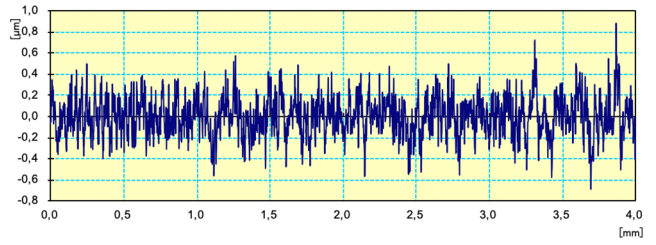


Fig. 13. Exemplary surface roughness profile plot of the samples after anodisation at 300 V

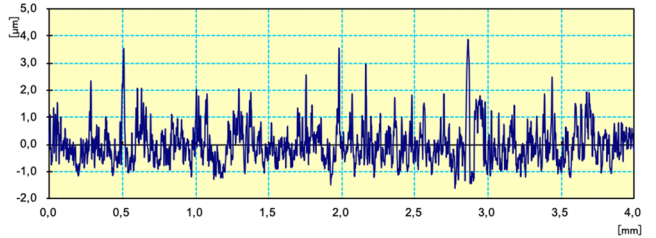


Fig. 14. Exemplary surface roughness profile plot of the samples after anodisation at 350 V

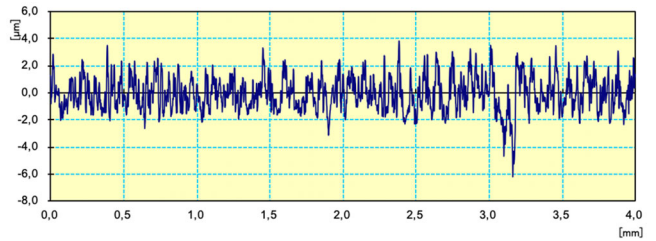


Fig. 15. Exemplary surface roughness profile plot of the samples after anodisation at 400 V

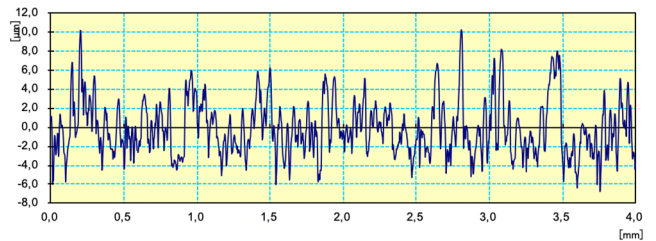


Fig. 16. Exemplary surface roughness profile plot of the samples after anodisation at 450 V

In Figures 17-23, exemplary appearances of the liquid droplets used for measurements are presented. Table 4 provides the results of the contact angle measurements.

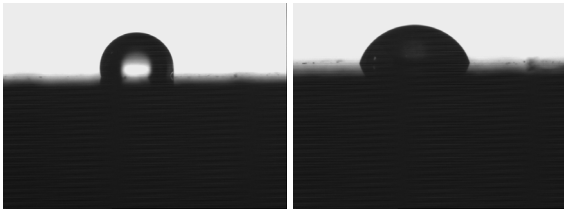


Fig. 17. Image of water droplet (left side) and diiodomethane droplet (right side) on the surface anodised at 200 V

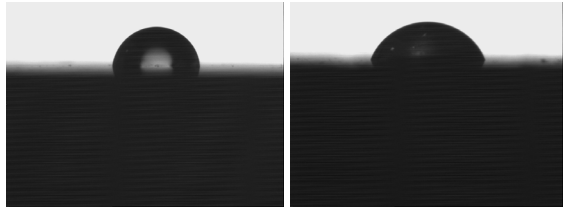


Fig. 18. Image of water droplet (left side) and diiodomethane droplet (right side) on the surface anodised at 230 V

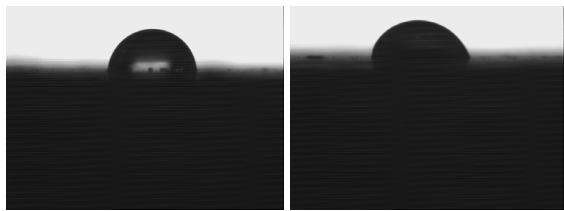


Fig. 19. Image of a water droplet (left side) and diiodomethane droplet (right side) on the surface anodised at 270 V

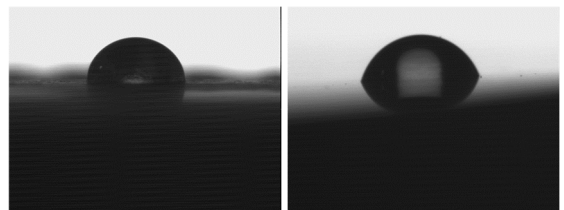


Fig. 20. Image of water droplet (left side) and diiodomethane droplet (right side) on the surface anodised at 300 V

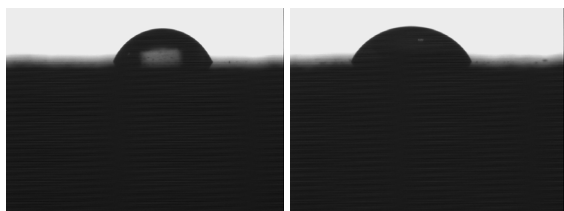


Fig. 21. Image of water droplet (left side) and diiodomethane droplet (right side) on the surface anodised at 350 V

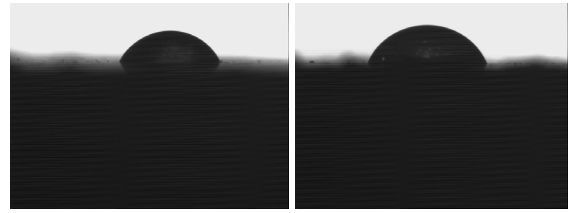


Fig. 22. Image of water droplet (left side) and diiodomethane droplet (right side) on the surface anodised at 400 V

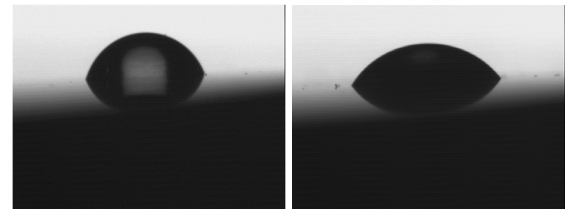


Fig. 23. Image of water droplet (left side) and diiodomethane droplet (right side) on the surface anodised at 450 V

Table 4.

Results of contact angle measurements on the surface using water droplets

Anodising voltage, V	water		diiodomethane	
	Mean	XD	Mean	XD
200	105.1	2.4	67.3	1.2
230	87.0	0.9	65.7	0.8
270	77.0	2.6	61.7	3.1
300	70.8	2.7	53.2	1.7
350	53.3	1.7	41.0	1.8
400	52.9	3.0	38.0	0.5
450	47.1	0.6	30.6	1.3

Based on the presented images and data from Table 4, it can be observed that with an increase in anodising voltage, the wettability of the coatings increases for both water and diiodomethane.

Conducted research demonstrated the possibility of obtaining anodised oxide layers on titanium with a thickness ranging from 0.65 μm to 13.2 μm . Those layers exhibit both crystalline and partially amorphous structures. With increasing anodising voltage, the surfaces became more developed with increased indentation and undercut features. Other researchers have made similar observations using anodisation with H_2SO_4 and H_3PO_4 solutions, indicating the correlation between anodising voltage and layer thickness [18,20,24]. SEM cross-sectional analysis also revealed a similar correlation between increased layer thickness and applied voltage. The obtained layers showed close adhesion

to the titanium surface. Furthermore, it was confirmed that the anodising voltage, rather than the duration of the process, influenced the layer thickness, consistent with the findings of previous studies by Delplancke J-L et al. and LeClere DJ et al. [21,22]. The easy and rapid voltage control appears to be more precise and repeatable compared to high-temperature methods, avoiding errors in abrasive treatment mentioned by Gołębiowski [23].

Chemical composition analysis of the surface confirmed the presence of titanium and oxygen in all tested samples. Additionally, the presence of silicon was observed, which can be attributed to its passage from the anodising electrolyte. Perhaps it contributes to the formation of the amorphous phase since previous studies using pure H_2SO_4 and H_3PO_4 solutions did not identify the presence of the amorphous phase [18,20,24]. During the process, silicon was incorporated into the oxide layer. It is consistent with earlier studies where sulfuric acid was used as the electrolyte, resulting in the presence of sulphur in the formed layer [18]. Similarly, in another study, the use of orthophosphoric acid led to the incorporation of phosphorus [24]. Since those authors did not detect the presence of the amorphous phase, it is possible that silicon was incorporated as silica (SiO_2).

The formation of surface indentations and the developed titanium surface are relevant regarding the retention of applied dental porcelain. Obtained layers exhibit a beneficial porous structure. Adjusting the anodising voltage appropriately allows the layer thickness and pore size to be controlled, as confirmed by the microscopic images of the surfaces and cross-sections. However, it should be noted that there is a certain threshold thickness beyond which the mechanical properties of the layers significantly decrease. The optimal thickness, also observed in cobalt and nickel alloys, ranges from 0.5 to 1 μm [17]. The presence of pores allows the liquid ceramic material to flow in during firing, positively affecting the quality of the bond between the oxides in the ceramic and titanium oxide, facilitating their mutual dissolution during the initial stages of firing. However, the influence of silicon incorporated into the layer on the subsequent bonding between the dental porcelain and the titanium is difficult to estimate. If we assume it is silica, considering it is an oxide, its interaction with the porcelain should be beneficial. Taking into account the potential use of those layers as intermediates during ceramic firing (similar to cobalt and nickel-based prosthetic alloys), the best option appears to be the layer obtained at an anodising voltage of 270 V. The obtained coatings are not too thick, which should maintain good adhesion, and after ceramic firing, they provide sufficient strength for the bond between the ceramic and the titanium. In addition to the appropriate

thickness, those layers also possess roughness, which should enhance the mechanical interlocking of the liquid ceramic within the surface irregularities. Both the vertical and horizontal roughness parameters seem sufficient to allow the flow of liquid porcelain during the firing process.

Furthermore, the favourable wetting of the anodised surface by both polar (water) and non-polar (diiodomethane) liquids is crucial in applying and firing dental porcelain. Since the ceramic applied to the metal substrate is a water-based suspension, good wetting by polar liquids ensures its proper spreading on the surface. During firing, the water from the applied suspension evaporates, and after ceramic melting, it becomes a non-polar liquid. In this case, good wetting by non-polar liquids will guarantee proper flow in the surface irregularities.

5. Conclusions

1. The best option, in terms of the connection between the metal substrate and the veneering ceramic, appears to be anodisation at a voltage of 270 V.
2. To determine the suitability of anodisation in the studied solution, further investigations on the bond strength between the veneering ceramic and the anodised titanium are necessary.

References

- [1] I.A. Tsolakis, S. Gizani, A.I. Tsolakis, N. Panayi, Pedodontic Appliances: A Critical Review of a New Era for Treatment, *Child* 9/8 (2022) 1107. DOI: <https://doi.org/10.3390/children9081107>
- [2] D.F. Williams, On the mechanisms of biocompatibility, *Biomaterials* 29/20 (2008) 2941-2953. DOI: <https://doi.org/10.1016/j.biomaterials.2008.04.023>
- [3] D.F. Williams (ed), *Definitions in biomaterials: proceedings of a consensus conference of the European Society for Biomaterials*, Chester, England, March 3-5, 1986, vol. 4, Elsevier, New York, 1987.
- [4] P. Downarowicz, M. Mikulewicz, Trace metal ions release from fixed orthodontic appliances and DNA damage in oral mucosa cells by in vivo studies: A literature review, *Advances in Clinical and Experimental Medicine* 26/7 (2017) 1155-1162. DOI: <https://doi.org/10.17219/acem/65726>
- [5] H.-H. Huang, Y.-H. Chiu, T.-H. Lee, S.-C. Wu, H.-W. Yang, K.-H. Su, C.-C. Hsu, Ion release from NiTi orthodontic wires in artificial saliva with various

- acidities, *Biomaterials* 24/20 (2003) 3585-3592. DOI: [https://doi.org/10.1016/S0142-9612\(03\)00188-1](https://doi.org/10.1016/S0142-9612(03)00188-1)
- [6] K. Banaszek, L. Klimek, Ti(C, N) as barrier coatings, *Coatings* 9/7 (2019) 432. DOI: <https://doi.org/10.3390/coatings9070432>
- [7] K. Banaszek, A. Wiktorowska-Owczarek, E. Kowalczyk, L. Klimek, Possibilities of applying Ti (C, N) coatings on prosthetic elements - Research with the use of human endothelial cells, *Acta of Bioengineering and Biomechanics* 18/1 (2016) 119-126. DOI: <https://doi.org/10.5277/ABB-00220-2014-04>
- [8] K. Banaszek, L. Klimek, J.R. Dąbrowski, W. Jastrzębski, Fretting wear in orthodontic and prosthetic alloys with Ti(C, N) coatings, *Processes* 7/12 (2019) 874. DOI: <https://doi.org/10.3390/pr7120874>
- [9] D. Quadras, U. Nayak, N. Kumari, H. Priyadarshini, S. Gowda, B. Fernandes, In vivo study on the release of nickel, chromium, and zinc in saliva and serum from patients treated with fixed orthodontic appliances, *Dental Research Journal (Isfahan)* 16/4 (2019) 209-215.
- [10] I. Sifakakis, T. Eliades, Adverse reactions to orthodontic materials, *Australian Dental Journal* 62/S1 (2017) 20-28. DOI: <https://doi.org/10.1111/adj.12473>
- [11] P.I. Brånemark, U. Breine, R. Adell, B.O. Hansson, J. Lindström, A. Ohlsson, Intra-osseous anchorage of dental prostheses: I. Experimental studies, *Scandinavian Journal of Plastic and Reconstructive Surgery* 3/2 (1969) 81-100. DOI: <https://doi.org/10.3109/02844316909036699>
- [12] M. Klekotka, J.M. Dąbrowski, K. Rećko, Fretting and Fretting Corrosion Processes of Ti6Al4V, *Materials* 13/7 (2020) 1561. DOI: <https://doi.org/10.3390/ma13071561>
- [13] M. Gołębiowski, A. Sobczyk-Guzenda, W. Szymański, L. Klimek, Influence of parameters of stream abrasive treatment of titanium surfaces on contact angle and surface free energy, *Inżynieria Materiałowa - Materials Engineering* 31/4 (2010) 978-980 (in Polish).
- [14] P. Haag, K. Nilner: Bonding between titanium and dental porcelain: a systematic review, *Acta Odontologica Scandinavica* 68/3 (2010) 154-164. DOI: <https://doi.org/10.3109/00016350903575260>
- [15] O. Inan, A. Acar, S. Halkaci, Effects of sandblasting and electrical discharge machining on porcelain adherence to cast and machined commercially pure titanium, *Journal of Biomedical Materials Research Part B: Applied Biomaterials* 78B/2 (2006) 393-400. DOI: <https://doi.org/10.1002/jbm.b.30500>
- [16] K. Banaszek, K. Pietnicki, L. Klimek, The influence of parameters of abrasive jet machining processing on the number of stubble elements stuck in nickel-chrome alloy surface, *Inżynieria Materiałowa - Materials Engineering* 32/4 (2011) 312-315 (in Polish).
- [17] I. Al Hussaini, K.A. Al Wazzan, Effect of surface treatment on bond strength of low-fusing porcelain to commercially pure titanium, *The Journal of Prosthetic Dentistry* 94/4 (2005) 350-356. DOI: <https://doi.org/10.1016/j.prosdent.2005.07.007>
- [18] M. Wilk, L. Klimek, Oxide layers on titanium obtained by anodization in sulphuric acid, *Metal Forming* 30/2 (2019) 135-144.
- [19] L. Benea, E. Mardare-Danaila, M. Mardare, J-P. Celis, Preparation of titanium oxide and hydroxyapatite on Ti-6Al-4V alloy surface and electrochemical behaviour in bio-simulated fluid solution, *Corrosion Science* 80 (2014) 331-338. DOI: <https://doi.org/10.1016/j.corsci.2013.11.059>
- [20] D. Capek, M-P. Gigandet, M. Masmoudi, M. Wery, O. Banakh, Long-time anodisation of titanium in sulphuric acid, *Surface and Coatings Technology* 202/8 (2008) 1379-1384. DOI: <https://doi.org/10.1016/j.surfcoat.2007.06.027>
- [21] J.-L. Delplancke, R. Winand, Galvanostatic anodization of titanium - I. Structures and compositions of the anodic films, *Electrochimica Acta* 33/11 (1988) 1539-1549. DOI: [https://doi.org/10.1016/0013-4686\(88\)80223-8](https://doi.org/10.1016/0013-4686(88)80223-8)
- [22] D.J. LeClere, A. Velota, P. Skeldon, G.E. Thompson, S. Berger, J. Kunze, P. Schmuki, H. Habazaki, S. Nagata, Tracer Investigation of Pore Formation in Anodic Titania, *Journal of The Electrochemical Society* 155/9 (2008) C487. DOI: <https://doi.org/10.1149/1.2946727>
- [23] M. Gołębiowski, K. Pietnicki, L. Klimek, Influence of parameters of air abrasion on the number of abrasive particles embedded in the surface of titanium alloy, *Magazyn Stomatologiczny - Dental Magazine* 20/6 (2010) 34-38 (in Polish).
- [24] M. Wilk, L. Klimek, Oxide layers on titanium obtained by anodizing in orthophosphoric acid, *Archives of Materials Science and Engineering* 94/1 (2018) 11-17. DOI: <https://doi.org/10.5604/01.3001.0012.7803>



© 2023 by the authors. Licensee International OCSCO World Press, Gliwice, Poland. This paper is an open-access paper distributed under the terms and conditions of the Creative Commons Attribution-NonCommercial-NoDerivatives 4.0 International (CC BY-NC-ND 4.0) license (<https://creativecommons.org/licenses/by-nc-nd/4.0/deed.en>).